Measurement and Analysis of UWB-IR Antenna Performance for WPANs

Sathaporn Promwong[♰♦], Wataru Hanitachi[♰], Jun-ichi Takada[♰], Pichaya Supanakoon[♦] and Prakit Tangtisanon[♦]

[♰]Graduate School of Science and Engineering,
Tokyo Institute of Technology
O-okayama Minami 6 Bldg., 2-12-1, O-okayama, Meguro-ku, Tokyo 152-8552, Japan.
E-mail: {ken,takada}@ap.ide.titech.ac.jp

[♦]Department of Information Engineering, Faculty of Engineering,
King Mongkut's Institute of Technology Lat Krabung, Bangkok 10520, Thailand.
E-mail: {kspichay,ktprakit}@kmitl.ac.th

Abstract

In ultra wideband impulse radio (UWB-IR) transmission systems, the direction of transmission has a significant effect on system design and performance. Moreover, the effects of distortion due to the antennas are not negligible and affects the link budget estimation. The link budget of the free space propagation loss is usually estimated by using Friis' transmission formula. However, it is not directly applicable to the UWB radio transmission systems, in particular the single band impulse radio, as the formula is expressed as a function of the frequency. In this paper, we evaluate the transmission of UWB antennas for wireless communication. An experiment of the transfer function of the transmitter and receiver antennas are done using biconical antennas and the measurements are covered by using a vector network analyzer (VNA). The measurement data are used to evaluate the UWB transmission gain based on the extended Friis' transmission formula. The matched filter reception is considered to maximize the SNR at the receiver for evaluation. This technique gives very accurate results and is very useful for the design and evaluation of UWB impulse radio transmission systems.

Keywords: UWB-IR, UWB antennas, Ultra wideband, Friis' transmission formula, Impulse radio

1. Introduction

Ultra wideband (UWB) radio technology is an ideal candidate that can be utilized for commercial, shot-range, low power, low cost indoor communication systems such as Wireless Personal Area Networks (WPANs) [1]-[3].

In UWB communication systems, the antennas are significant pulse-shaping filters. Any distortion of the signal in the frequency domain causes the distortion of the transmitted pulse shape. Consequently, this will increase the complexity of the detection mechanism at the receiver [4]. The antenna design for UWB signal radiation is one of the main challenges [5]-[7]. Especially, low cost, geometrically small and still efficient structures are required for typical wireless applications such as WPANs.

Even if the channel is in line of sight (LOS), the Friis transmission formula cannot be directly applied to the UWB radio as the bandwidth of the pulse is extremely wide. Furthermore, simple comparison between waveforms of transmitter and receiver is not significant because of the distortion of the waveform caused by the frequency response of the antenna.

In this paper, we discuss free space transmission measurements of UWB antennas. This technique is based on the Friis' transmission formula, in the sense that we would like to derive the equivalent antenna gain for UWB systems. The transmission waveform and the matched filter reception are keys for the extension of Friis' formula to UWB. We carried out an experiment using a biconical antenna for UWB operation on the flat top of a roof.

2. Measurement Arrangement

In this section, some issues of the preparation for the experiments are described [8]:

2.1 Experiment Setup

A UWB radio channel transfer function was measured as S_{21} in frequency domain by using a vector network analyzer (VNA). The VNA was operated in the response measurement mode, where Port-1 was the transmitter (Tx) Port and Port-2 was the receiver (Rx) port, respectively. The measurement was done on the top of a building to simulate free space. Both Tx and Rx antennas were fixed at the height of 1.3 m and separated by 1 m. The setup is shown in Fig. 1.

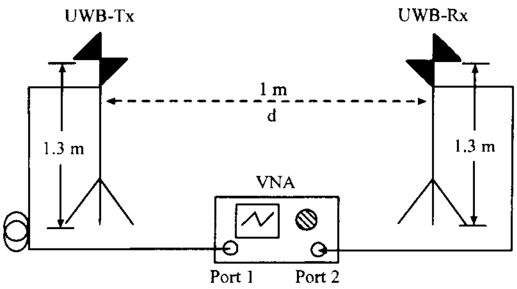

Fig 1. The experiment setup.

The difference of the free space propagation distance d does not affect the waveform distortion. For this reason, it was set to be $d = 1$ m in this simulation. The orientations of the two biconical antennas are shown in Fig. 2.

2.2 Antennas Under Test

In this study, we considered a broadband antenna that was suitable for the operation with pulsed waveforms [9]. We have chosen this biconical antenna for the ease of fabrication, as well as it is often used as a standard antenna. The geometry and the dimension of the antenna are shown in Fig. 3. The upper cone is connected to the RF signal while the lower cone is connected to ground. Figure 4 shows the reflection coefficient $|S_{11}|$ of the antenna feed point. From the figure, we can see that the reflection coefficient was below -10 dB in the frequency range between 3.1 GHz and 10.6 GHz.

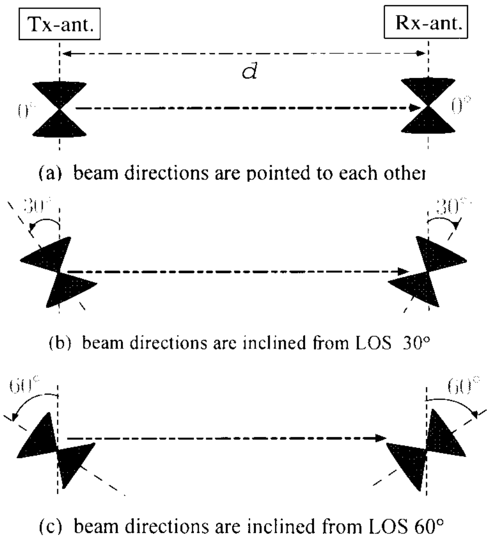

Fig. 2. Orientations of two biconical antennas.

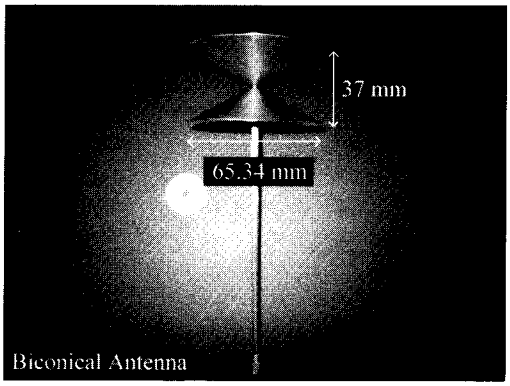

Fig 3. Geometry and dimensions of the biconical antenna.

In the S_{21} measurements, there are three different kinds of orientation as shown in Fig. 2. They are facing toward the same direction to each other so that $G_t = G_r$ is satisfied. The main beam resides in the xy-plane, i.e. omnidirectional pattern in Fig. 3. The antenna is also tilted as much as 30° and 60° along θ directions, as well as the main beam direction.

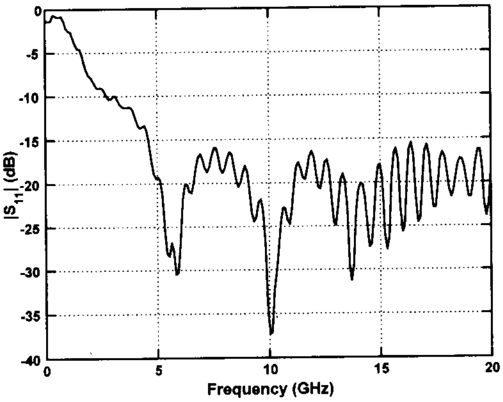

Fig 4. $|S_{11}|$ characteristics of biconical antenna.

2.3 Parameters of Experiments

The important parameters for the experiments are listed in Table 1.

Table 1. Experimental setup parameters.

Parameter	Value
Frequency range	3 to 11 GHz
Number of frequency points	1601
Dynamic power range	80 dB
Tx antenna height	1.3 m
Rx antenna height	1.3 m
Distance between Tx and Rx	1.0 m
Pointing angle	0°/30°/60°

It is noted that the calibration is done at the connectors of the cables to be connected to the antennas. Therefore, all the impairments of the antenna characteristics are included in the measured results.

2.4 UWB Signal Model

The effect of the waveform distortion is more obvious when the bandwidth is wider. We considered the impulse radio signal that fully covers the FCC band [10], i.e., 3.1~10.6 GHz. The center frequency and the bandwidth were therefore set to be f_0 =6.85 GHz and f_b =7.5 GHz, respectively. The transmission waveform assumed in the simulation was a single ASK pulse with the carrier frequency f_0. To satisfy the bandwidth requirement of f_b, the pulse length was set to be $2/f_b$. Then the signal was band-limited by a Nyquist roll-off filter with roll-off factor $\alpha = 0$ (rectangular window) and passband $(f_0 - f_b/2, f_0 + f_b/2)$. Figure 5 shows the transmission of pulse waveform. The transmission process of the pulse waveform is simulated based on the measured transfer function of the antenna.

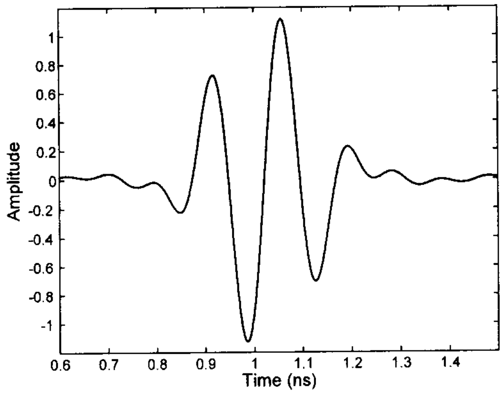

Fig 5. The transmission waveform of UWB signal

3. The Extension of Friis' Transmission Formula for Ultra Wideband Systems

In this study, we focus on the link budget evaluation in the free space.

In narrowband systems, the link budget of the free space propagation loss is usually estimated by using Friis' transmission formula [11], which has been widely used and can be applied to the calculation of these LOS channels.

$$G_{Friis} = \frac{P_r}{P_t} = G_f G_r G_t, \qquad (1)$$

where G_r and G_t are Rx and Tx antenna gain,

$$G_f = \left(\frac{\lambda}{4\pi d}\right)^2, \qquad (2)$$

is the free space propagation gain (less than unity in practice), $\lambda = c/f$ is the wavelength, c is the velocity of light, and f is the frequency.

It is noted, however, that Eq. (1) is satisfied only at certain frequencies, and is not directly applicable to UWB systems. We have recently proposed a new extension of the Friis' transmission formula to take into account the transmission signal waveform and its distortion as well [12].

The input signal $v_t(t)$ at the transmitter port is expressed as the convolution of an impulse and the pulse shaping filter h_t as:

$$v_t(t) = E_t\delta(t) * h_t(t), \qquad (3)$$

where

$$\int_{-\infty}^{\infty} h_t^2(t)dt = \int_{-\infty}^{\infty} |H_t(f)|^2 df = 1. \qquad (4)$$

Friis' formula is extended taking into account the transmission waveform as:

$$H_{e-Friis}(f) = \frac{V_r(f)}{E_t} = H_f H_t \mathbf{H}_r \cdot \mathbf{H}_t, \qquad (5)$$

where

$$\mathbf{H}_a = \mathbf{H}_a(\theta_a, \varphi_a, f),$$
$$= \hat{\theta}_a \mathbf{H}_{a\theta}(\theta_a, \varphi_a, f) + \hat{\varphi}_a \mathbf{H}_{a\varphi}(\theta_a, \varphi_a, f), \qquad (6)$$

$a = r$ or t,

is a complex transfer function vector of the antenna relative to the isotropic antenna,

$$H_f = \frac{\lambda}{4\pi d}\exp(-jkd), \qquad (7)$$

is the free space transfer function where

$$k = \frac{2\pi}{\lambda}, \qquad (8)$$

is the propagation constant. Unit vectors $\hat{\theta}_a$, $\hat{\varphi}_a$ to express the polarization are defined with respect to the local polar coordinates of each of the antennas. The following relations can be easily derived:

$$\hat{\theta}_r = \hat{\theta}_t, \qquad (9)$$

$$\hat{\varphi}_r = -\hat{\varphi}_t, \qquad (10)$$

At the receiver, the matched filter $H_{MF}(f)$ is introduced to maximize the signal-to-noise ratio (SNR) of the receiver output, as shown in Fig. 6:

$$H_{MF}(f) = \frac{H^*_{e-Friis}(f)}{\sqrt{\int_{-\infty}^{\infty} |H_{e-Friis}(f)|^2 df}}, \qquad (11)$$

which satisfies the following constant noise output power condition :

$$\int_{-\infty}^{\infty} |H_{MF}(f)|^2 df = 1. \qquad (12)$$

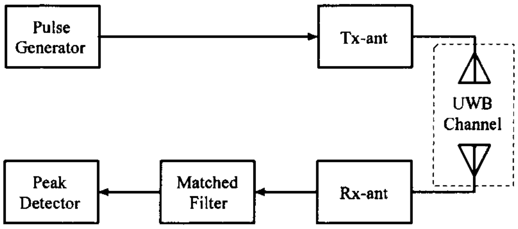

Fig 6. Block diagram of transmission system for the extension of Friis' transmission formula to treat UWB signals.

When we assume E_t, which is the amplitude of impulse input that generates transmission signal $v_t(t)$, is 1, the waveform and the spectrum of the receiver output are $h_{e-Friis}(t)$ and $H_{e-Friis}(f)$, respectively. The waveform of output from the matched filter $v_{MF}(t)$ and the spectrum of output from the matched filter $V_{MF}(t)$ are:

$$v_{MF}(t) = h_{e-Friis}(t) * h_{MF}(-t);$$
$$= \frac{h_{e-Friis}(t) * h_{e-Friis}(-t)}{\sqrt{\int_{-\infty}^{\infty} h_{e-Friis}^2(t)dt}}, \qquad (13)$$

$$V_{MF}(f) = H_{e-Friis}(f)H_{MF}(f),$$
$$= \frac{|H_{e-Friis}(f)|^2}{\sqrt{\int_{-\infty}^{\infty} |H_{e-Friis}(f)|^2 df}}, \qquad (14)$$

taking its maximum at $t = 0$ as:

$$\max_t v_{MF}(t) = v_{MF}(0) = \int_{-\infty}^{\infty} V_{MF}(f)df,$$
$$= \sqrt{\int_{-\infty}^{\infty} |H_{e-Friis}(f)|^2 df}. \qquad (15)$$

Equation (15) is the UWB extension of Friis' transmission formula. This equation includes three elements, i.e., the frequency characteristics of the antennas, the frequency characteristics of free space propagation, and the spectrum of the transmission signal.

4. Results of Experiments

Figures 7 and 8 show the amplitude and the phase of the transfer function measured for three different antenna setups. From Fig. 7, the radiation pattern seems to change from frequency to frequency, which may result in waveform distortion.

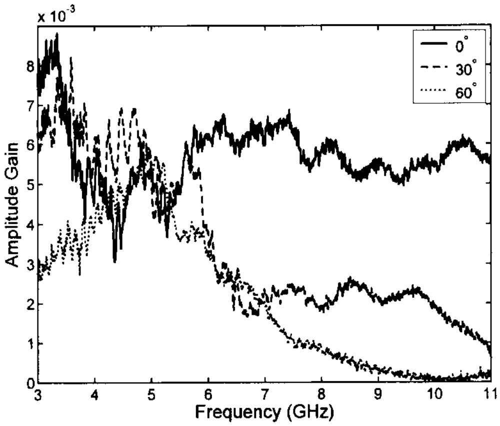

Fig 7. Measured transfer functions for different antenna pointing conditions: amplitude.

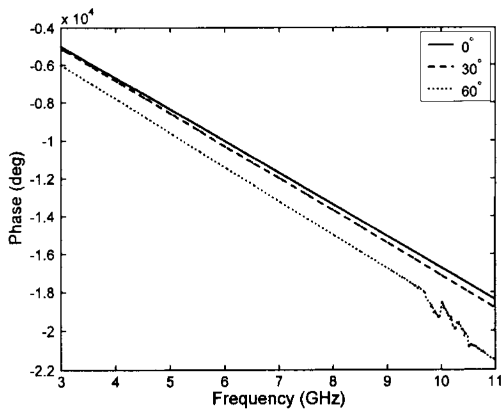

Fig 8. Measured transfer functions for different antenna pointing conditions: phase.

Figure.9 shows the received pulse waveforms when the transmission waveform shown in Fig. 5 is input. For comparison, the waveform for isotropic antennas is shown as "Free Space". Compared with the isotropic case, the pulse waveform is very much distorted and lengths become longer.

Although the accurate transfer function of each individual antenna is measured using three-antenna methods, Figs. 10 and 11 show the approximate antenna transfer functions which are obtained by assuming that Tx and Rx antennas are identical. The vertical axis is normalized by the isotropic antenna. Therefore, for 0° and 30° positions, the directive gain is below 0 dB for almost frequency range.

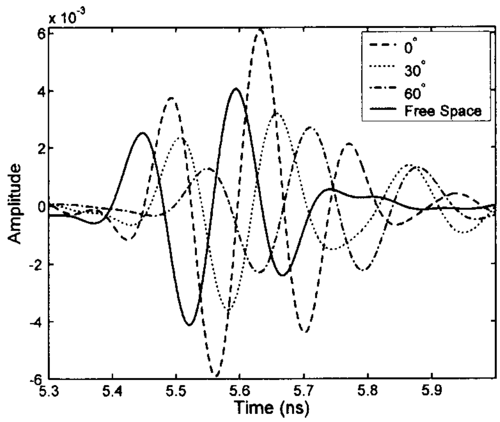

Fig 9. Received waveform at the antenna output.

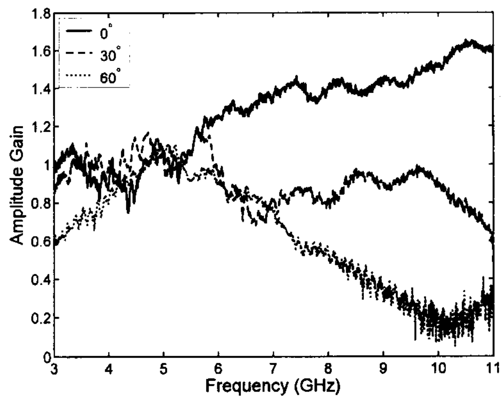

Fig 10. Antenna transfer function: amplitude.

Figures.12 and 13 show the output of matched filters. In Fig. 12, the matched filter is optimized for the each individual scenario, and the results correspond to the maximum available gain. In contrast, for Fig. 13, the matched filter is replaced by that for isotropic antennas. This result is more realistic in practice, because the directions of the Tx and Rx antennas are not usually arbitrarily controllable, but set at convenient positions.

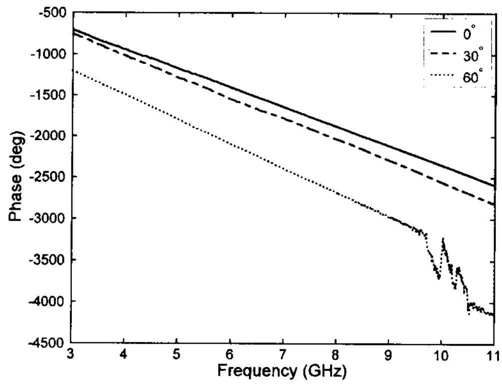

Fig 11. Antenna transfer function: phase.

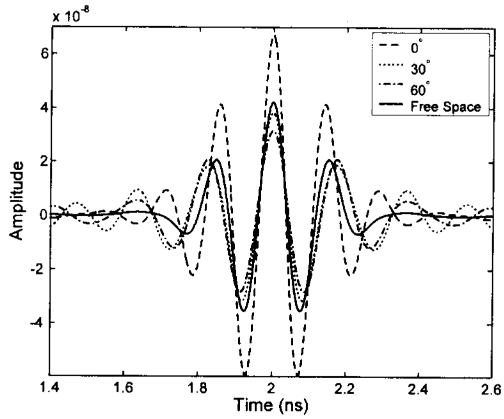

Fig 12. Output of matched filter: optimal.

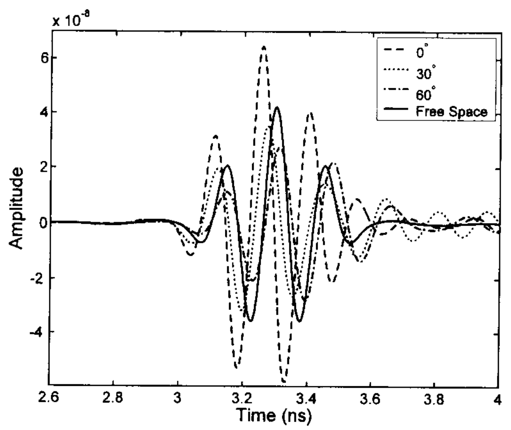

Fig 13. Output of matched filter: free space approximation.

Table 2 summarizes the overall gain with respect to the isotropic antennas case. Since the gain at most of the frequencies was below unity, the dB value of the gain is negative. By using the approximate matched filter, the gain has been degraded.

Table 2. Relative gain of (antenna + matched filter), with respect to the ideal isotropic antennas.

Filter	Gain (dBi)		
	0°	30°	60°
Optimum	3.6	-0.8	-2.7
Isotropic approximation	3.2	-1.6	-3.7

As the amount of the gain degradation depends on the setup, Table 3 lists the correlation coefficient of the impulse responses between the received signal and the approximate matched filter using the isotropic antennas. For the case of 60°, the correlation coefficient is low compared with others. This is partly the reason why gain degradation by using the approximate matched filter is larger only for this case.

Table 3. Correlation coefficient between the impulse response of the received signal and the approximate matched filter by using isotropic antennas.

Orientation	0°	30°	60°
Correlation coefficient	0.96	0.91	0.86

5. Conclusion

In this paper, we discussed the measurement and analysis of ultra wideband antenna performance. In the proposed scheme, Friis' transmission formula is extended in order to take into account the transmit waveform and the matched filter of the system. An experimental demonstration using a biconical antenna for UWB was shown, and the specific gain value could be obtained for the Tx and Rx antenna pair.

We introduced the matched filter for the optimum receiver. However, if the distorted component should be regarded as interference, the equalizer instead of the matched filter will be used. Even in this case, a similar discussion can be done on the definition of the gain. To know the individual antenna parameters, three-antenna measurements will be done.

This scheme is applicable for the evaluation of various UWB antennas. Therefore, some typical UWB antennas will be evaluated by using the proposed technique.

6. Acknowledgement

This research is partly supported by the fund from the Telecommunications Advancement Organization (TAO) of Japan.

7. References

[1] K. Siwiak, Ultra-Wide Radio: Introducing a New Technology, 2001 Spring IEEE Veh. Tech. Conf. (VTC), Plenary session, May 2001.

[2] K. Siwiak, Ultra-Wide Radio: The Emergence of an Important RF Technology, Proc. 2001 Spring IEEE Veh. Tech. Conf. (VTC), May 2001.

[3] J. Farserotu, A. Hutter, F. Platbrood, J. Gerrits, A. Pollini, UWB Transmission and MIMO Antenna Systems for Nomadic User and Mobile PAN, Wireless Personal Commun., No.22, pp.197-317, 2002.

[4] K. Siwiak, Impact of UWB Transmission on Generic Receiver, Proc. IEEE Veh. Tech. Conf. (VTC), May 2001.

[5] H. Schantz, Measurement of UWB Antenna Efficiency, Proc. IEEE Veh. Tech. Conf. (VTC), May 2001.

[6] H.F. Harmuth and S. Ding-Rong, Antennas for Nonsinusiodal Wave-Part I: Radiators, IEEE Trans. Elec. Mag. Compat., Vol. EMC-25, No.1, pp.13-24, Feb. 1983.

[7] H.F. Harmuth and S. Ding-Rong, Antennas for Nonsinusiodal Wave Part II: Sensors, IEEE Trans. on Elec. Mag. Compat., Vol. EMC-25, No.1, No.2, pp.107-115, May 1983.

[8] S. Promwong, W. Hachitani, J. Takada, and P. Tangtisanon, Experimental Evaluation of the Free Space Transmission Characteristics of UWB Antenna, IEICE Rep., AP 2003-42/SAT 2003-34/MW 2003-48/OPE 2003-35, pp.7-12, July 2003.

[9] M.K.Y. Lai, A.L. Sinopoli and W.D. Burnside, A Novel Antennas for Ultra-Wideband Applications, IEEE Trans. Antennas Propagat., Vol.AP-40, No.7, pp. 755–760, July 1992.

[10] Federal Communications Commission, Revision of Part 15 of the Commission's Rules Regarding Ultra-Wideband Transmission Systems, First Report and Order, FCC 02-48, Apr. 2002.

[11] H.T. Friis, A Note on a Simple Transmission Formula, Proc. IRE, Vol. 34, No.5, pp.254-256, May 1946.

[12] J. Takada, S. Promwong, and W. Hachitani, Extention of Friis' Transmission Formula for Ultra-Wideband Systems, IEICE Tech. Rep., WBS2003-8/ MW 2003-20, pp. 45-50, Sagamihara, Kanagawa, May 2003.